International Journal of Geo-Information

MDPI

Article

A Methodology for Planar Representation of Frescoed Oval Domes: Formulation and Testing on Pisa Cathedral

Andrea Piemonte [1,*,†], Gabriella Caroti [1,†], Isabel Martínez-Espejo Zaragoza [1,†], Filippo Fantini [2,†] and Luca Cipriani [2,†]

1 Civil and Industrial Engineering Department (DICI), University of Pisa, Largo Lucio Lazzarino 1, 56122 Pisa, Italy; gabriella.caroti@unipi.it (G.C.); isaroju@gmail.com (I.M.-E.Z.)
2 DA–Dipartimento di Architettura, Alma Mater Studiorum Università di Bologna–Bologna, Viale del Risorgimento, 2, 40136 Bologna, Italy; filippo.fantini2@unibo.it (F.F.); luca.cipriani@unibo.it (L.C.)
* Correspondence: andrea.piemonte@unipi.it; Tel.: +39-050-221-7773
† These authors contributed equally to this work.

Received: 8 June 2018; Accepted: 3 August 2018; Published: 7 August 2018

Abstract: This paper presents an original methodology for planar development of a frescoed dome with an oval plan. Input data include a rigorous geometric survey, performed with a laser scanner, and a photogrammetry campaign, which associates a high-quality photographic texture to the 3D model. Therefore, the main topics include the development of geometry and, contextually, of the associated textures. In order to overcome the inability to directly develop the surface, an orthographic azimuthal projection is used. Starting from a prerequisite study of building methodology, the dome is divided into sectors and bands, each linked with the maximum acceptable deformations and the actual geometric discontinuities detectable by the analysis of Gaussian curvature. Upon definition of the development model, a custom automation script has been devised for geometry projection. This effectively generates a (u,v) map, associated to the model, which is used for model texturing and provides the planar development of the fresco.

Keywords: frescoed vault; planar representation of vault; cultural heritage documentation

1. Introduction

The availability of large-scale planar representations of frescoes painted on curved surfaces provides useful support for restoration and maintenance operators. During operations related to diagnostics and restoration and/or maintenance of frescoes, specialized operators document the status quo and each intervention in technical forms, providing rationale for the decisions and stating the steps of the intervention that leads to the final result. Such documentation includes an explanatory report and 2D documents, both graphical and photographical, for each step at an adequate scale. In addition, these documents form a relevant archival knowledge base which, when used in conjunction with the parent 3D model, can provide the foundation for reconstruction of disrupted or destroyed heritage. In order to generate 3D models incorporating metrically exact geometries and high-quality photo-realistic textures, it is possible to integrate two well-established surveying technologies—Terrestrial Laser Scanning (TLS) and photogrammetry [1,2]. TLS enables fairly consistent geometric precision for any given scanner surface range, irrespective of the surface texture of the object. On the other hand, photogrammetry exploits cameras and image collection techniques so as to achieve high-resolution, high chromatic quality textures.

Advances in digital photogrammetry, in particular Structure from Motion (SfM) and Multi-View Stereo (MVS), ensure good results, even with extreme image taking conditions that are otherwise unusable in analogue or analytical photogrammetry [3].

The potential offered by current photogrammetric methodologies allows the exploitation of historic photographic archives in order to register archive images on up-to-date models and reconstruct destroyed or severely damaged frescoes [4] as well as supplying visitors of cultural heritage sites with augmented reality solutions capable of overlaying contents on a digital representation of a work of art [5].

Upon the generation of textured models of curved surfaces, a further problem involves their best planar representation, reducing or at least controlling the ensuing deformations.

This problem involves two distinct issues:

- performing the development (more appropriately termed as projection and pseudo-development for non-directly developable surfaces) of geometric shapes;
- applying a reference system (u,v) to geometric shapes in order to retain their association with textures.

While the literature provides several suggestions to solve the first issue, some of which have already been implemented in CAID (Computer Aided Industrial Design) software, there are only a few implementations that partially solve the second problem with applications such as Technodigit3DReshaper and the open-source Cloud Compare [6]. Planar representation of geometric shapes must therefore differentiate between developable and non-developable curved surfaces. Developable surfaces can be "unfolded" on a plane without any deformation. This operation is bijective and can be reversed with no loss of accuracy [7].

Planar representation of non-directly developable surfaces requires their projection on a plane or other developable auxiliary surfaces. This operation is typical of cartographic representations, where the Earth's surface is approximated to an ellipsoid and projected on a plane. Such projections, however, entail some linear, angular, or area deformations. While no projection can completely remove these deformations, it is possible to check their dimension and keep it within given tolerance ranges by means of adequate precautions, which often provide reduction of the projected surface area and repetition of the projection with different auxiliary surfaces.

Unlike previous contributions, the present work aims to define a methodological approach for planar pseudo-development of a frescoed dome with oval-plan design and polycentric sections.

The object of study is the dome of Pisa Cathedral (Figure 1), figuring a fresco depicting the Assumption of the Virgin Mary with several saints, painted between 1627 and 1630 by Orazio Riminaldi [8].

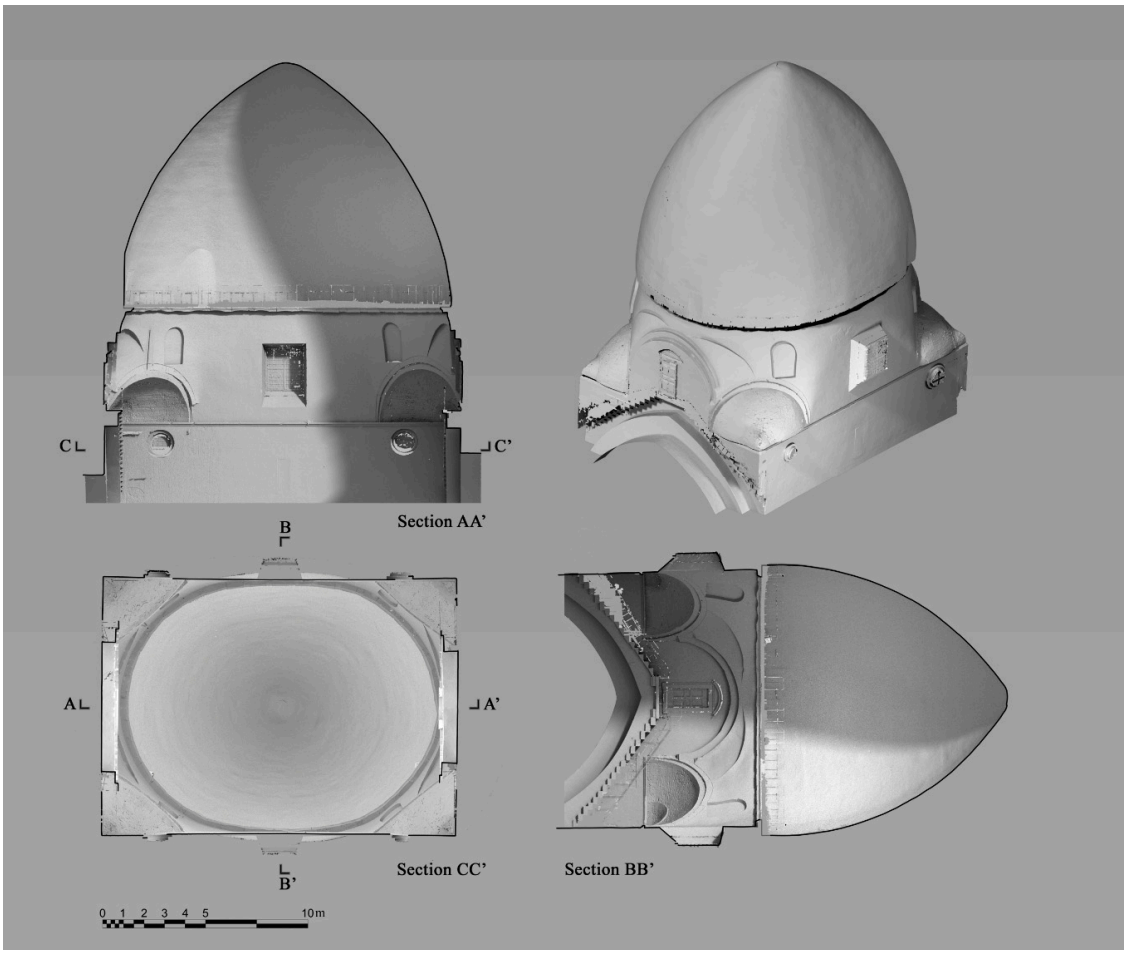

Figure 1. Frescoed dome, Pisa Cathedral.

2. Materials

The dome of Pisa Cathedral dates back to the early twelfth century and presents an original shape compared to the European panorama of the time. As pointed out by Piero Sanpaolesi [9], who worked as superintendent in Pisa between 1943 and 1960, a clear typological interpretation is a prerequisite when carrying out studies on the domes of historic buildings. There are two types of domes: extrados ones (*cupole estradossate*) and the pseudo-cupulas (or "corbelled", or "horizontal rings"). Pisa Cathedral dome belongs to the first category, which has a curvilinear profile of the extrados similar to that of the intrados (the volume of the cupula can be considered as the result of a "shift" of the intrados surface outside).

This is a departure from the technical solutions adopted in other buildings such as the Pantheon in Rome which, seen from the outside, hides for the most part the hollow spherical volume of the intrados inside a heavy cylinder made of bricks. In other terms, in the first case, the extrados is dimensioned by means of a simple offsetting operation of the intrados surface, i.e., the internal and external shapes coincide, with the respective positions differing by a value homogeneously defined in the design and execution phase.

In the second case, inside and outside shapes present different, independent shapes; an inside semi-sphere externally corresponds to a "lowered", flatter profile, such as in the Pantheon in Rome. According to Sanpaolesi, the example supplied by the Pisan dome is one of the first examples in Europe and in the Mediterranean Basin in which the form perceived internally is also visible externally, forgoing the heavy and massive stereometry that characterizes the drums of many previous buildings, in particular of the classical era. The domes belonging to the latter category, in fact, base their strength

on the progressive decrease in thickness as well as the weight of the construction materials, ring after ring. In addition to the already mentioned and iconic Pantheon in Rome, numerous mausoleums built in the Imperial era and late Antiquity [10], such as the Mausoleum of Sant'Elena, are characterized by the same feature, i.e., the internal and external shapes do not match.

In the specific case of the Cathedral of Pisa, the shape of the plan at the impost height is oval; this feature makes this constitutive element incompatible with a revolved surface, as occurs in numerous previous examples, also belonging to the classical age, e.g., the Temple of Diana in Baia [11–13].

The original impetus that characterized the original shape of the Pisan dome was reduced by ancient restorations, in particular by the addition of a small loggia built starting from 1389 for the next seven years by Puccio di Landuccio and Lapo di Gante based on a model [9]. The small loggia appears to have had the function of a reinforcing hoop aimed at containing horizontal thrusts through an elegant colonnade that increased the vertical component of the forces. Similar strategies were also adopted by architects for the restoration of ancient buildings as in the case of the previously mentioned Mausoleum of Sant'Elena with the raising of the upper drum, which incorporated the original tiered cornice [10]. The loggia follows the irregular octagonal profile of a drum but leans on a series of coeval arches, whose purpose was the unloading of forces along the eight angular pillars.

Surveying

Currently, 3D architectural surveys mainly rely on two modeling methodologies—range-based and image-based [14]. The former exploits TLS to provide 3D point cloud models made of millions of points framed in a common reference system, which can represent the survey object geometry with subcentimeter accuracy [15]. The second technique—through the integration of efficient computer vision algorithms such as SfM and MVS with classic photogrammetry procedures—can provide both a geometric model and the radiometric information needed for model texturing [16].

Given the need to obtain a model of the dome ensuring both the strict geometric definition of its shapes and the analysis of the fresco, it was necessary to proceed with both surveying methods and to integrate their output [1,2].

The possibility of placing surveying instrumentation in close proximity of the survey object, together with the visual interference of the internal scaffolding during its staging, led to planning distinct steps for the geometry survey:

1. Topographical survey of a support network, at ground level.
2. Laser scanning and photogrammetry of the intrados, at ground level.
3. Laser scanning and photogrammetry of the intrados, at matroneum level.
4. Topographical survey of an internal support network, at springer level.
5. Laser scanning and photogrammetry of the intrados, at springer level.

Completion of steps 1 to 3 took place prior to the staging of scaffolding. Steps 4 and 5 were completed during a temporary work stoppage, with the internal scaffolding at springer level.

As previously stated, while the scaffolding does provide a privileged access point to upper levels, it intrinsically lacks the stability required for precision surveys. For this reason, the support survey carried out by total station is of utmost importance. Throughout its execution, measuring stations were consistently placed on steady spots, such as ground, matroneum floor, and masonry landings along stair flights linking service doors at drum and springer level.

Points surveyed via total station acted as either Ground Control Points (GCPs) or Check Points (CPs) in photogrammetric processing and point cloud registration; GCPs were used for scaling and georeferencing the model, and CPs were used to control its accuracy.

As for TLS surveys—performed via Leica's C10 ScanStation with a point cloud density of about 70 pts/cm^2 on average—point clouds from lower level scans included both the area of interest, i.e., the dome, and portions closer to the ground. These clouds were orientated using ground-level benchmarks, which provided higher reliability than those at dome level. Registration of clouds

collected in close proximity to the dome relied on both dome-level benchmarks and cloud-matching algorithms with previously registered clouds.

Photogrammetric surveying—carried out by means of Nikon's D700 DSLR fitted with a 50 mm lens at dome level and an 85 mm lens at matroneum and ground levels—yielded a mean Ground Sampling Distance (GSD) of 3 mm. Image processing via SfM algorithms require an overlap of more than 70%. Acquisition of images taken from different distances (12 m at dome drum level, 45 m at ground level) allowed for model checking and increased rigidity. Bundle adjustment was performed with 10 GCPs and yielded a standard deviation of 2 mm based on 15 CPs.

Based on these values, images were correctly orientated in the relevant reference system and therefore could be used for texturing TLS models registered in a common reference system.

3. Methods

3.1. Geometry Pseudo-Development

Rieck et al. [7] provided an in-depth study of unfolding methodologies for high-resolution 3D meshes of objects with rotation symmetry. Previous photogrammetry works used cylinders for the development of 3D surfaces having a precise analytical representation [17]. The use of map-like projections has already proved effective for the achievement of raster images of frescoes painted on arches or spherical surfaces [18,19]. A thorough discussion of the development methods for spherical objects can be found in the cartographic literature [20]. In later works, arbitrary surfaces were interpolated with triangle strips prior to their development [21]. Bevilacqua et al. [22] provided an example of planar representation of a fresco painted on an "*a schifo*" vault for which the error for planar projection was checked.

The methodology adopted for the planar representation of the dome can be described as an orthographic azimuthal projection (Figure 2). In this kind of projection, linear deformation Δ_L for a given curvature radius is directly linked to the distance of the projected point relative to the tangency point of the plane and therefore to the angle α, according to Equation (3):

$$\left|\hat{CP}\right| = R \cdot \sin\alpha \tag{1}$$

$$\left|\overline{CP'}\right| = R \cdot \sin\alpha \cdot \cos\alpha \tag{2}$$

$$\Delta_L = R \cdot \sin\alpha \cdot (1 - \cos\alpha) \tag{3}$$

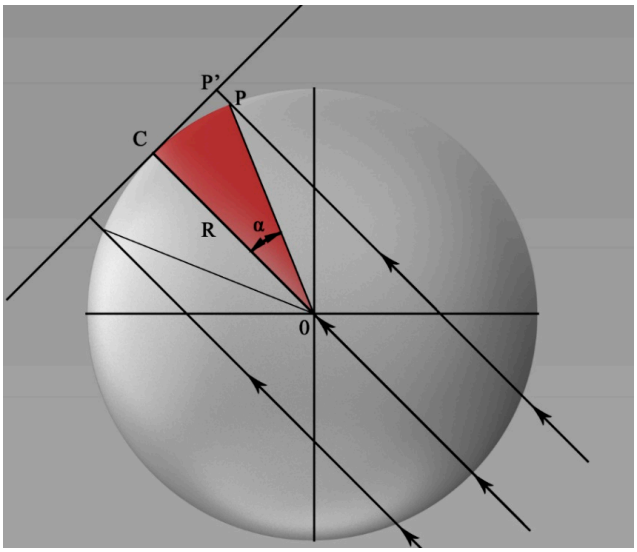

Figure 2. Geometric diagram of orthographic azimuthal projection.

Due to its double curvature, together with variable curvature radius for both meridian and horizontal sections, the surface was split into zones and bands in order to reduce linear deformations for the points farthest away from the tangency point on the projection plane, resulting, in fact, as a whole in a polycentric orthogonal azimuthal projection. As regards the fuses, the choice of their number directly affects the fragmentation of the final representation; for this reason, it is advisable to keep the greatest amplitude compatible with the final scale and the related allowable deformation. As regards the bands, reducing their extent does not affect representation quality or processing time, thanks to a custom script, which will be discussed later.

Processing included use of algorithms belonging to distinct application fields (photogrammetry, reverse modeling, polygonal modeling) and the development of a script aimed at the automation of iterated operations required for the pseudo-development of the dome intrados.

A rapid, intuitive way to assess the developable nature of surfaces requires the use of Gaussian maps, which evaluates the curvature at any point for the main directions of the surface. Given any planar curve, it is possible to define the tangent, the normal, and the osculating circle for any of its points, with the inverse of the radius of the osculating circle being the curvature k [23]:

$$k = \frac{1}{R} \tag{4}$$

For 3D surfaces, these concepts apply as follows: For any point, it is possible to define the normal, the tangent, and infinite curvatures, i.e., one for each section curve obtained by the intersection of a plane containing the normal. Notable among these are the main curvatures $k1$ and $k2$—the maximum and the minimum—which can be positive or negative, based on the accordance with the normal. Gaussian curvature is defined by:

$$k = k1 \cdot k2 \tag{5}$$

It is therefore possible to obtain the following cases:

1. simple curvature surfaces: $k1 = 0$, $k2 \neq 0$; or $k1 \neq 0$, $k2 = 0$.
2. double curvature surfaces: $k1 \neq 0$, $k2 \neq 0$.

Developable surfaces can only have one curvature, i.e., when $k = k1 \cdot k2 = 0$.

The sign of Gaussian curvature is also useful for shape definition:

1. $k > 0$ define ellipsoids, which can be concave ($k1 > 0$ and $k2 > 0$) or convex ($k1 < 0$ and $k2 < 0$);
2. $k = 0$ further distinguishes between $k1 = k2 = 0$ (plane) and either $k1$ or $k2 \neq 0$ (cylinder);
3. with $k < 0$, the two main curvatures have opposite signs, identifying a saddle surface.

In 3D modeling applications based on Non Uniform Rational Basis-Splines (NURBS), it is possible to visualize the Gaussian curvature of a shape in order to immediately perceive if, and in which areas, this is developable.

In the case of a morphologically complex digital model—obtained by laser scanning—it is logical to expect that the numerous irregularities due to superficial alterations, structural settlements, and restorations lead to an unclear reading of the Gaussian curvature. For these reasons, the Pisa dome is a case in point, as it requires particular arrangements in order to undergo Gaussian curvature analysis and understand which parts of its shape is developable and which are not, to provide a possible solution for the development.

The essential first phase is the achievement of a NURBS representation from the TLS mesh in order to carry out the Gaussian curvature analysis expressed through a visual output in false colors directly on the model. This step of the process involves reverse modeling techniques to convert the intrados—made of triangles—into a boundary representation (B-Rep) formed by parametric patches. False colors on a connected set of NURBS patches supply the user with precise information on the location of developable areas—displayed in green by the application used in this work (approximately

equivalent to cones or cylinders, $k = 0$). The aim is to obtain "heuristic" clues to be used in the following steps.

3.2. Geometry Pseudo-Development

There are numerous ways for obtaining a mathematical model from a high-detail mesh. Each system has its pros and cons regarding lead times and overall metric reliability of the model obtained through reverse modeling techniques [24] compared to the original mesh and, last but not least, an easy portability of the model towards a NURBS application.

(1) Direct patching: Direct patching—present in all the reverse modeling applications, such as 3D Systems Geomagic Design X or InnovmetricPolyWorks—was deemed not suitable, although they are highly automated and faster than the other strategies examined (Figure 3).

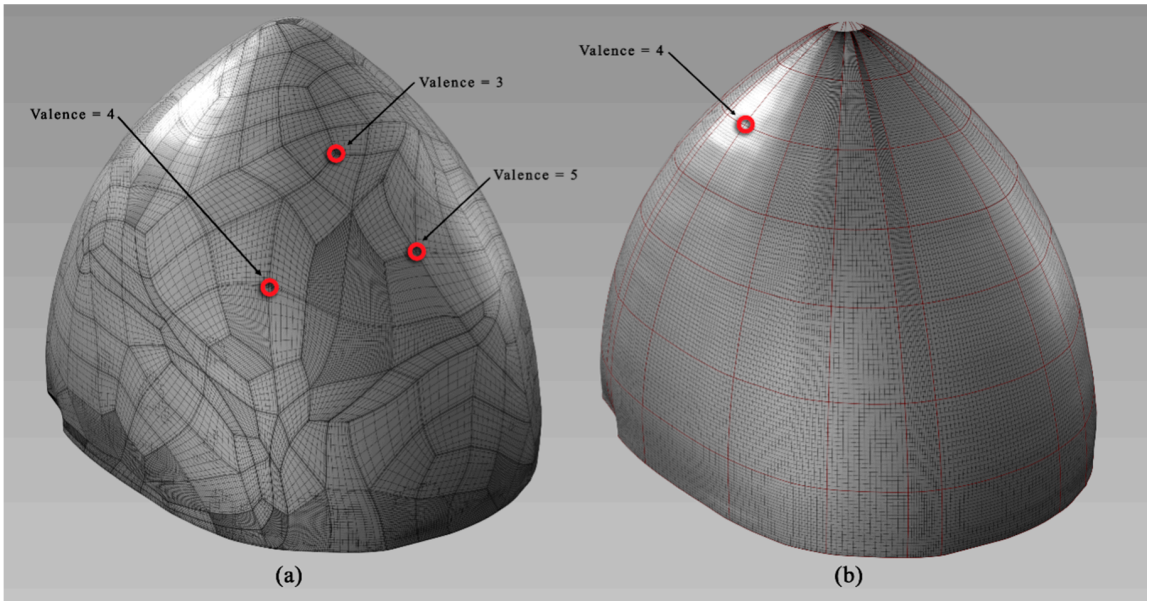

Figure 3. (**a**) Automated direct patching; (**b**) supervised 3D patching.

The main reason is that the set of NURBS patches "covering" the high-density mesh is obtained through a series of customizable parameters that are unreliable for both constructive and design features of the dome. In Figure 3a, the automatic procedure results in discontinuous and interrupted sequences of loops of edges; in addition, patch organization is neither horizontal, nor meridian. In fact, boundary vertices belonging to the patches do not have constant valence equal to four, which is the optimum for the next steps of the procedure. Regular horizontal and vertical rows and columns of patch would have matched the natural arrangement of bricks and ribs of the centring adopted for the dome, as shown in Figure 3b. The cupola was apparently built by arranging rows of horizontally laid bricks (consistent with the parallels) or normal to the surface of the intrados. Nevertheless, direct patching leads to an inconsistent arrangement with respect to the natural division into parallels and meridians of the dome. In fact, the automatic and seemingly random arrangement of the patches and the relative isoparametric curves (isoparms) makes it extremely difficult to obtain a 2D version of the whole B-Rep that is able to visually and intuitively respond to the needs of this study, i.e., interdisciplinary approach, collaborative work with restorers, etc.

In other words, the isoparametric curves, namely the graphic lines running along the surface in the U and V directions and giving shape to NURBS patches, do not fit with a constructive reading of the artifact.

(2) 3D Patch Network: This is an alternative strategy to obtain a NURBS model inside the already mentioned applications, and it consists of the combined use of reverse modeling techniques (section extraction and features) and is a procedure which, depending on the situation, can be highly automated or manual. Firstly, the technique involves the operation called "de-featuring", which leads to removal from the model the areas that hinder the continuity of the shape by integrating them with mesh in continuity with neighboring areas, in particular, holes and tiny dangling elements (like windows, niches, or overhanging parts). Once the surface has been normalized, the automatic, manual, or assisted identification of feature curves (generatrix and directrix) leads to the determination of a wireframe representation of the mesh model. In general, contiguous patches are constructed in such a way as to intersect in points of valence equal to 4, defined by the intersection of parallels and meridians.

(3) Direct modeling: This starts with a series of sections/feature curves. It presents some problems, among which the main one is the reliability of the final NURBS model in relation to the original, since the deviation between mesh and NURBS cannot be evaluated step-by-step as in reverse modeling techniques. Once a limited number of sections—characterized by a large number of poles—are imported inside applications such as McNeel Rhinoceros and Autodesk Alias, they have to undergo a simplification process since fewer poles are always a better solution for the achievement of a nice curvature of patches. Nevertheless, CAID applications implement less specific controls with respect to those present in reverse modeling software, when simplifying a spline. On the contrary, if the number of poles on splines is kept high, without any particular intervention, the generated model can be locally very reliable (around the curves extracted from the mesh) but overall less reliable in the areas of connection between the sections (patch quality can be poor and conflicting with development tools).

(4) Retopology: This solution is implemented inside several entertainment applications (Foundry Modo, PixologicZBrush, etc.), and it can be a manual or an automatic process [25,26] aimed at remeshing highly detailed triangular meshes into "quads", namely four-sided polygons. Certain advances that have recently been implemented in modeling tools, both NURBS and polygonal, allow the conversion of such quad-polygonal meshes into mathematical models [27].

This set of techniques and opportunities—all evaluated by the research group—led to the use of a personalized approach. The first step involved the use of the 3D Patch Network to obtain information on the Gaussian curvature; the second phase is based on the use of the spline curves extracted from the model in the previous step and used as generatrices and directrices in order to obtain a second simplified geometric model based on NURBS technology through commands able to keep low and uniform the number of isoparametric curves. Reverse modeling techniques enable a full control on the deviation introduced during the simplification process while maintaining the intersection of the curves in points of valence equal to four. This model is constructed in such a way as to allow a particular type of linear development that is functional to verifying the validity of the approach used with the subsequent steps that will be based on discrete models in quadrangular polygons.

3.3. Design Analysis and Constructive Issues

The reverse modeling steps (3D Patch Network) were based on a series of studies and verifications concerning design analysis and ancient construction techniques. Hypotheses on the oval-plan outline of the dome (ichnographia) benefit from the new instrumental survey outcomes and verified hypotheses by Sanpaolesi who had already identified the centers and the curvature radii at the dome's impost plane—a polycentric curve identified by a series of modules (Figure 4).

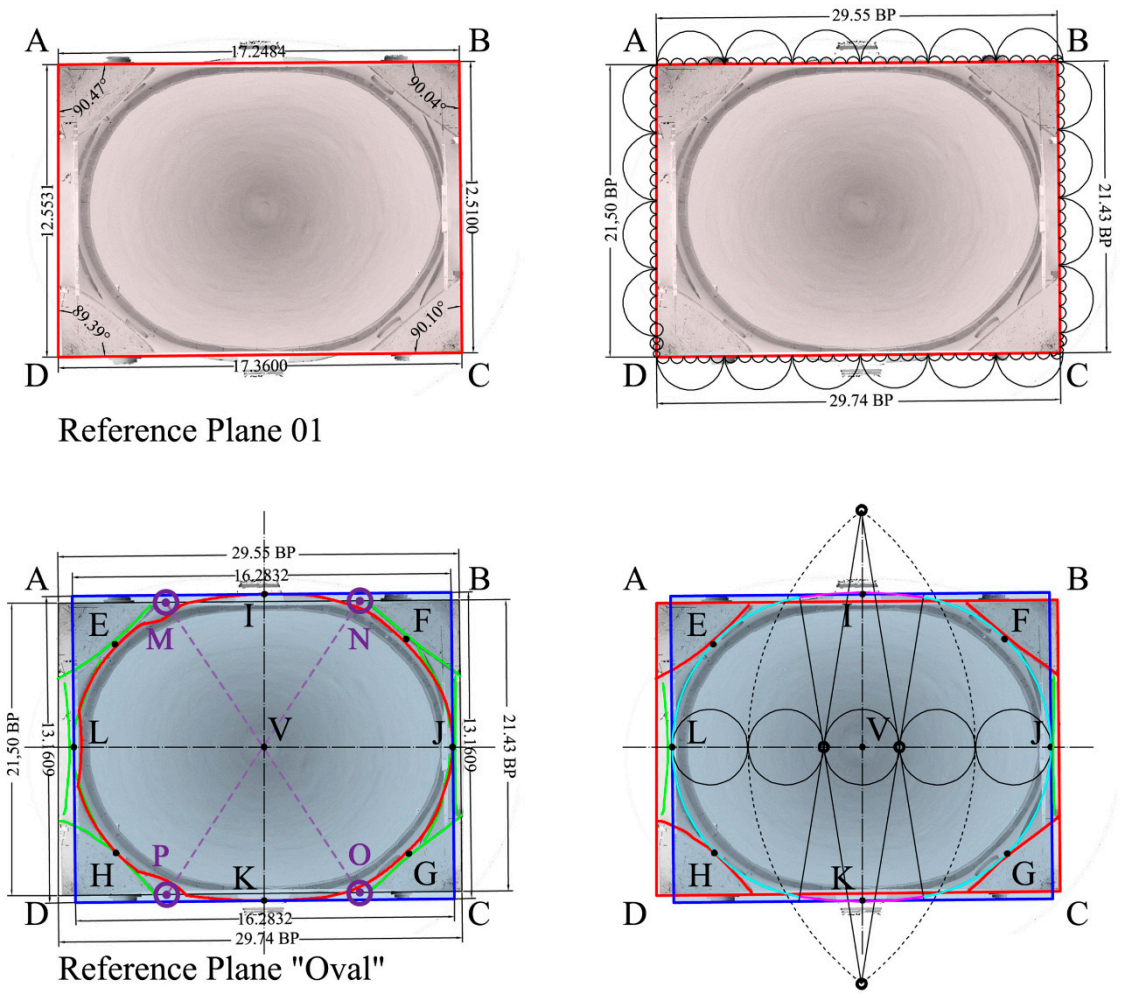

Figure 4. Design analysis and hypotheses on oval-plan outline. The main lengths are in both meters and ancient measuring system Braccia Pisane (BP).

The use of similar techniques for obtaining oval curves had been known since antiquity to define the plan design of amphitheatres [28]. This "geometric algorithm" led to the achievement of a closed curve with continuity of position (G0), of tangency (G1), but not of curvature (G2). The problem of reverse modeling therefore needs to be carried out bearing in mind these assumptions of ancient mathematics and geometry applied to design and construction.

Designing and construction issues can be considered in these terms (limiting for the moment the analysis to the intrados); the irregular quadrilateral (ABCD in Figure 4) constitutes the starting shape from which the irregular octagon was found out. This form will contain the oval of the intrados, but the octagon does not inscribe its curvilinear shape.

The individual sides of the quadrilateral (ABCD) measure in meters: AB = 17.248, BC = 12.510, CD = 17.360, DA = 12.553. In Pisan arms (Braccia Pisane, BP) measuring 0.5836 m [29], the following measurements are obtained: AB = 29.55; BC = 21.43; CD = 29.74; DA = 21.50.

Observing the major axis and the minor axis of the oval, it is possible to notice how the first (LJ) is shorter than the long side of the underlying rectangle (ABCD), while the second (IK) comes out of the same "boundary" drawn by the quadrangular perimeter.

Therefore, the oval is not exactly inscribed; instead, its layout is obtained through a tangency relationship solely affecting points E, F, G, and H (belonging to the oblique sides of the irregular octagon). The tangency in E, F, G, and H is accurately achieved, taking into account the constructive difficulties and irregularities due to deformations induced by phenomena of deterioration and

subsidence of the foundation and elevated structures occurring over nine centuries of life of the building [14].

These considerations have a possible construction-based explanation; when looking at the longitudinal section of the cathedral, overlapped with the plan, it is possible to understand the reason of this "shift" between the octagon and the bounding box of the oval (in blue in Figure 4).

When locating the main support points for temporary structures (centring), the architects of the cathedral should have opted for the minor axis of the oval. At the same time, they had to exploit the structural continuity of the piers from the first order to the compact connection masonry of the drum. Possibly, they placed the main ribs of the wooden centring in the areas between the oval and the ABCD rectangle, in particular near the points M, N, O and P (Figure 4).

It is presumable that additional ribs, probably of secondary importance, were laid on these two main arches following the same operating logic—the exploitation of intersection areas between the irregular octagon and the blue square in Figure 4.

For the ichnografia, it is still valid to assume what was claimed by Sanpaolesi [9], who proposed a polycentric curve based on the division of the major axis of the oval into five modules (Figure 4).

3.4. Segmentation of the Cupola

By executing a series of horizontal contour lines of the intrados surface, it is possible to obtain further information that is useful for carrying out a geometric and structural reading functional to the development of the intrados.

The field of geometric modeling provides two types of surfaces—primary and secondary—or blends [30]. In this study, this criterion was applied to perform a segmentation of the model useful for the purposes of this investigation, i.e., to subdivide a complex shape into several subsets coherent with the design and construction of the dome.

The primary surfaces are attributable to geometric primitives (plane, box, sphere, cone, etc.), while the secondary ones are used to connect two primary surfaces with zones of "passage", also referred to as blends [24]. By restricting the analysis to contour lines and not to the entire morphology, major discontinuities visible to the naked eye are evident, and they lead to the identification of two sets of curves: "primary" (type 1 and type 2 in Figure 5a) in continuity with the Sanpaolesi hypothesis and "secondary" (joints 1, 2, 3, 4). This is a first segmentation of the model to detect the most suitable sectors for development:

1. Two sectors (type 1 in Figure 5a): shapes formed by contour lines with minor curvature.
2. Two sectors (type 2 in Figure 5a): shapes formed by contour lines with greater curvature.
3. Four connecting sectors ("Joint" in Figure 5a): shapes formed by contour lines approximated to linear segments.

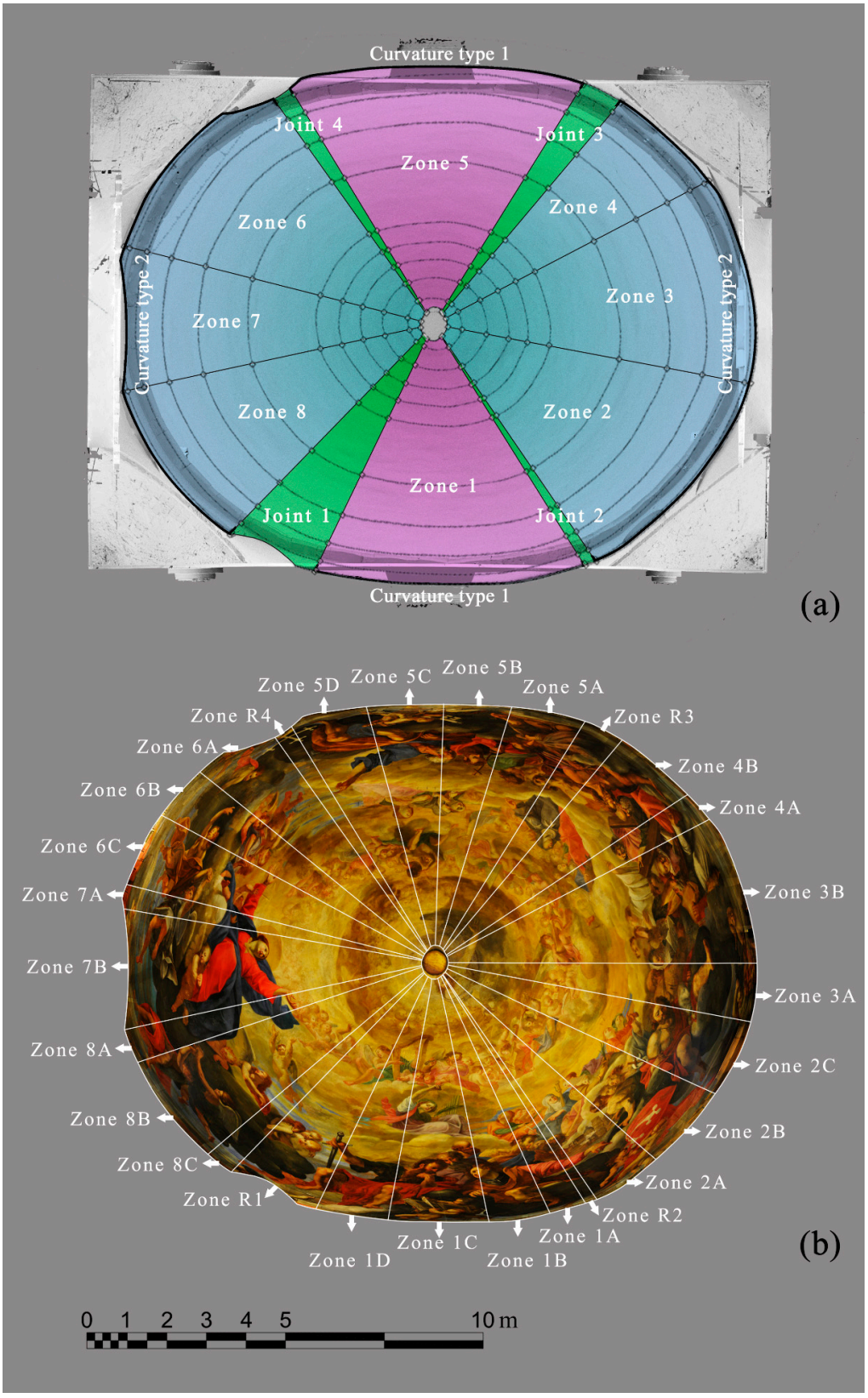

Figure 5. (**a**) Dome main zones subdivision; (**b**) Dome secondary zones subdivision.

In turn, these sectors can be further divided (second partition) on the basis of the variation of the Gaussian curvature (Figure 6) that identifies the overall trend of the surface and provides information about the areas to be subjected to specific shape analysis by means of the curvature graph.

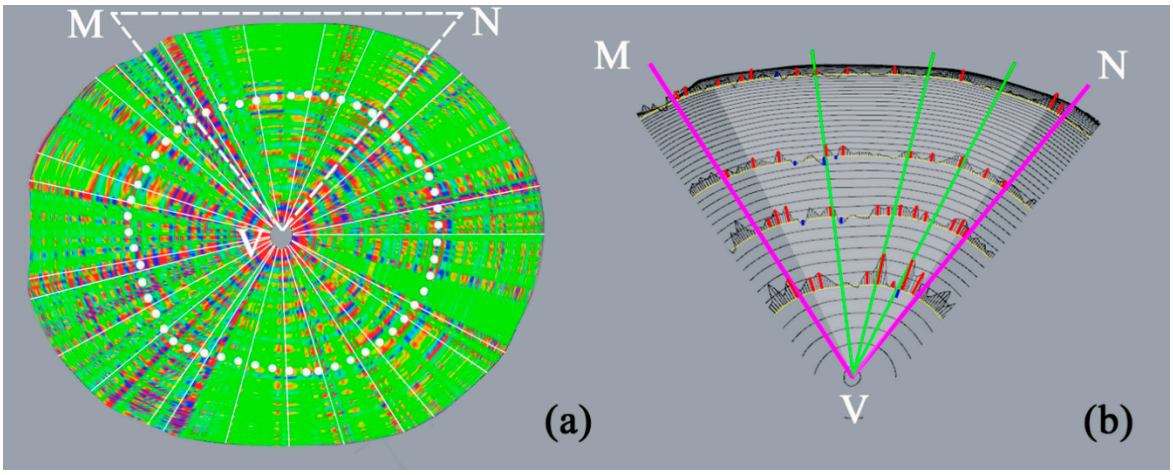

Figure 6. (**a**) Gaussian curvature analysis; (**b**) Zoom on MNV sector.

The subdivision of the main sectors into further parts of smaller extension responds to the need to reduce the deformations which, in an orthographic projection, increase as the distance of the projected element increases from the point of tangency of the plane on which the projection takes place.

Instead of making a subdivision based solely on the acceptable size of the area to be developed, the method chosen was aimed at defining additional discontinuity lines by comparing the trends deduced by curvature flow.

In general terms, the dome is composed of "locally developable" surfaces (green colored areas in Figure 6). However, at the height of 8.70 m—with respect to the impost line—a white-dotted contour line underlines a sudden change of Gaussian curvature sign. Above this curve, developable areas decrease significantly.

To illustrate the segmentation method used and applied in all sectors, the portion of the dome included in the MNV triangle is examined (Figure 6b).

The method is based on the analysis of 4 sample curves. One of them is the white-dotted contour line, which represents the "watershed" between areas that are more suitable for development and those that are not; two curves are above this threshold line; and just one curve is below since the area closer to the drum is for the most part colored in green (developable). The method to identify the "fine" partition is based on the following criteria shown in Figure 6:

1. identification in the macro-sector of positive "peaks" of the curvature (red color);
2. identification of areas with low and constant curvature (blue);
3. identification of inflection point areas (change from concave to convex, or vice versa): blue color abruptly alternated with red.

From these considerations, there derives a segmentation proposal for the oval dome into 8 main parts, in turn subdivided into 26 parts (Figure 5b). These 26 secondary zones have extension characteristics able to guarantee linear deformations compatible with a representation scale of 1:100, once having undergone an azimuthal-orthographic-polycentric projection (according to Equation (3) for a radius of curvature, equal to the maximum one found equal to 17 m).

Moreover, since these areas can be approximated in accordance with Gaussian curvature values to cylindrical or conical surfaces, some of the tools have already been implemented in geometric modeling software for the achievement of a pseudo-development of these geometric shapes.

For the modeling aimed at development, the widely used McNeel's Rhinoceros application (https://www.rhino3d.com) was used, since it provides the user with tools useful for the tests carried out.

The first is the possibility of developing continuous NURBS "patches" with Gaussian curvature equal to zero.

On the other hand, the development implemented in the application leads to the creation of a new 3D model belonging to the horizontal reference plane (X, Y), presenting a different parameterization with respect to its "original" 3D version (different number of isoparametric in the u and v direction). The reparametrization of the developed model represents a significant variation of the initial model structure—a variation in the number of nodes that govern the flow of the NURBS surface. In fact, it is a different model, with some properties in common with the original one.

However, the development tool has some tolerances and therefore manages to develop—within certain, not clearly definable, limits—surfaces with curvature $k \neq 0$ unless the structure of the isoparametric curves is regular (low number and homogeneous distribution of poles).

An additional tool gives the possibility of measuring models to evaluate the degree of reliability of the development operation. This essentially means measurement of lengths, areas, and angles in 2D and 3D.

Another aspect that must be pointed out is that it does not make NURBS modeling compatible with rigorous development intended for texturing operations aimed at supplying the user with some bitmap-type 2D output. In fact, the native-born parameterization of NURBS models does not correspond to a geometric development of the model into the (u,v) parameter space; the parametrized version of the NURBS model into the u and v dominion cannot be modified or altered since it is strictly functional to modeling. On the contrary, in polygonal models (born without parametrization), the creation of a one-to-one function that correspond a 3D shape makes to a 2D representation in (u,v) parameter space is facilitated by a range of tools [23].

Therefore, the NURBS application will be used only and exclusively for obtaining a boundary representation of the intrados of the dome; this will be realized starting from 26 curves lying on vertical planes obtained within the application of reverse modeling and mutually connected through the loft tool, which keeps the number of piece parameters low (Figure 7).

As already mentioned, the texturing systems implemented in the Rhinoceros software allow a very simplified parametrization aimed at texturing with respect to the familiar tools implemented in other applications for entertainment. Therefore, it was necessary to continue the work by introducing a program belonging to this field.

The 26 NURBS patches were converted into the same number of polygonal surfaces in such a way that the sampling step is constant across the whole region (along u and v) and compatible with the reliability necessary for the present study. This was measured on the basis of deviation tools inside the reverse modeling application used in this paper.

The method developed for the pseudo-development by projection of patches is as follows:

1. Use of Rhinoceros to obtain the measurable surface for validation of the process and to determine whether it is developable or not. If it is not, a further partition of the piece is carried out according to the stated method.
2. Export of the single NURBS patches into a modeler equipped with a robust polygonal modeling kernel. The model is tessellated so as to maintain quadrangular topology, namely with all vertex valences equal to 4, with the only exception of the vertices forming part of the outer edge of the patch (valence equal to 2 or 3).
3. Projection of each piece in the parameter space (u,v) through a script.
4. Conversion of the (u,v) parameterized version into a mesh belonging to the reference system (x, y, z) and export towards NURBS modeling application.

5. 2D polygon mesh conversion—obtained from parameterization—into NURBS model. This process takes place through the transformation of each cell (polygonal) of an equivalent patch (NURBS). This way, it will be possible to check the metric reliability of the projection operation.
6. Model comparison and error evaluation— areas and lengths of the edges of the patch.

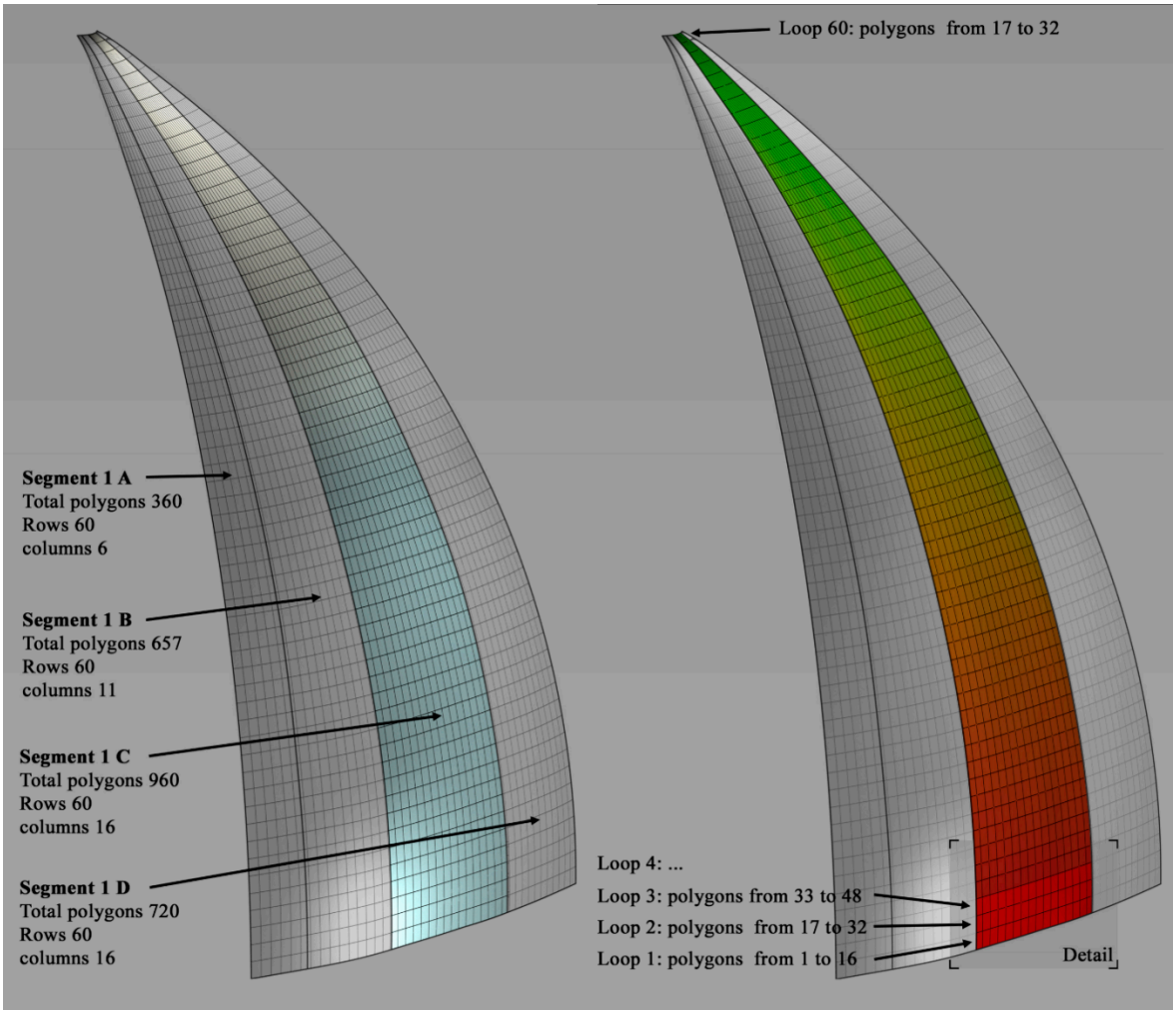

Figure 7. Portion of the dome included in MNV triangle.

3.5. Automatic Multicenter Orthographic Projection (AMOP) Script

The series of instructions aimed at developing has been carried out within the scripting system of The Foundry Modo and is based on the reiteration of a series of commands:

```
#LXMacro#
select.loop
workPlane.fitSelect
viewport.fit
tool.setuv.viewProj on
tool.apply
select.loopprev
workPlane.fitSelect
viewport.fitAlignSelected
tool.setuv.viewProj on
```

tool.apply
select.loopprev
workPlane.fitSelect
viewport.fitAlignSelected
tool.setuv.viewProj on
tool.apply

The purpose of the script is to automate the series of operations listed below and schematized graphically in Figure 8.

0. The necessary starting condition is that the model of each segment is displayed autonomously and in a single viewport, which must be strictly the orthographic view indicated with the name TOP (Top View). The first polygon in the lower left corner of the structured mesh of quadrangular polygons must be selected.
1. The script is launched, and it automatically selects the entire horizontal band of polygons (Belt 1): select.loop.
2. A drawing reference plane (UCS) is automatically set up; its normal vector is determined by the program through the average of the set of normals belonging to Belt 1, which we will call UCSBA1, i.e., UCS Belt Average 1: workPlane.fitSelect.
3. The initial TOP view (which allowed visualization of the segment from above) is now oriented in space in a congruent way with the normal outgoing from the plane defined by UCSBA1, which is centered on the selection together with the zoom value: viewport.fit.
4. A command is launched that makes a projection (central or parallel; in this case parallel) of the set of polygons selected in (x, y, z) onto the parameter space (u,v) using the view determined in the previous step: tool.setuv.viewProj on.
5. A one-to-one correspondence is established between the set of polygons of Belt 1 in (x, y, z) and an island in space (u,v): tool.apply.
6. The next band of polygons is automatically selected (Belt2): select.loop prev. From this point on, the sequence is repeated (Belt3, . . . , Beltn) until all the horizontal bands of polygons forming the segment are projected. These will appear superimposed in the parameter space (u,v) and therefore do not result as one-to-one correspondence with the whole set of points of the model in R3: a necessary and sufficient condition for correct texturing.
7. The biunique relationship is re-established by assigning $\forall$ Belt1, . . . , n a specific space in (u,v): uv.pack true false true auto 0.2 false false nearest 1001 0.0 -1.0 2.0 2.0.

Once this first phase is over, it is necessary to use a second script that automates the "recomposition" of islands corresponding to Belt1, . . . , n.

8. The first polygon on the bottom left is selected by the user that launches the second script that selects the entire horizontal band of polygons (Belt 1): select.loop.
9. The selection of Belt 1 is converted from polygons into edges: select.convert edge.
10. The one-to-one correspondence between the bands in R3 (Belt1, . . . , n) and their counterparts in (u,v) is not verified along the edges of the single islands of the Belts. The outlines of the islands are partly duplicated (see image) since they will belong to the previous and the next band. Since the program highlights this duplication, it is possible to exploit it to automate the "stitching" of the adjacent belts through the command: uv.sewMove select true.
11. From here on, the script repeats the operation of the previous point, changing first the selection filter: select.NextMode.
12. The next band is selected: select.loop next.
13. Upon merging all the belts into one island, a fitting is necessary in order not to extend the patch beyond the boundaries of the (u,v) space: uv.fit false.

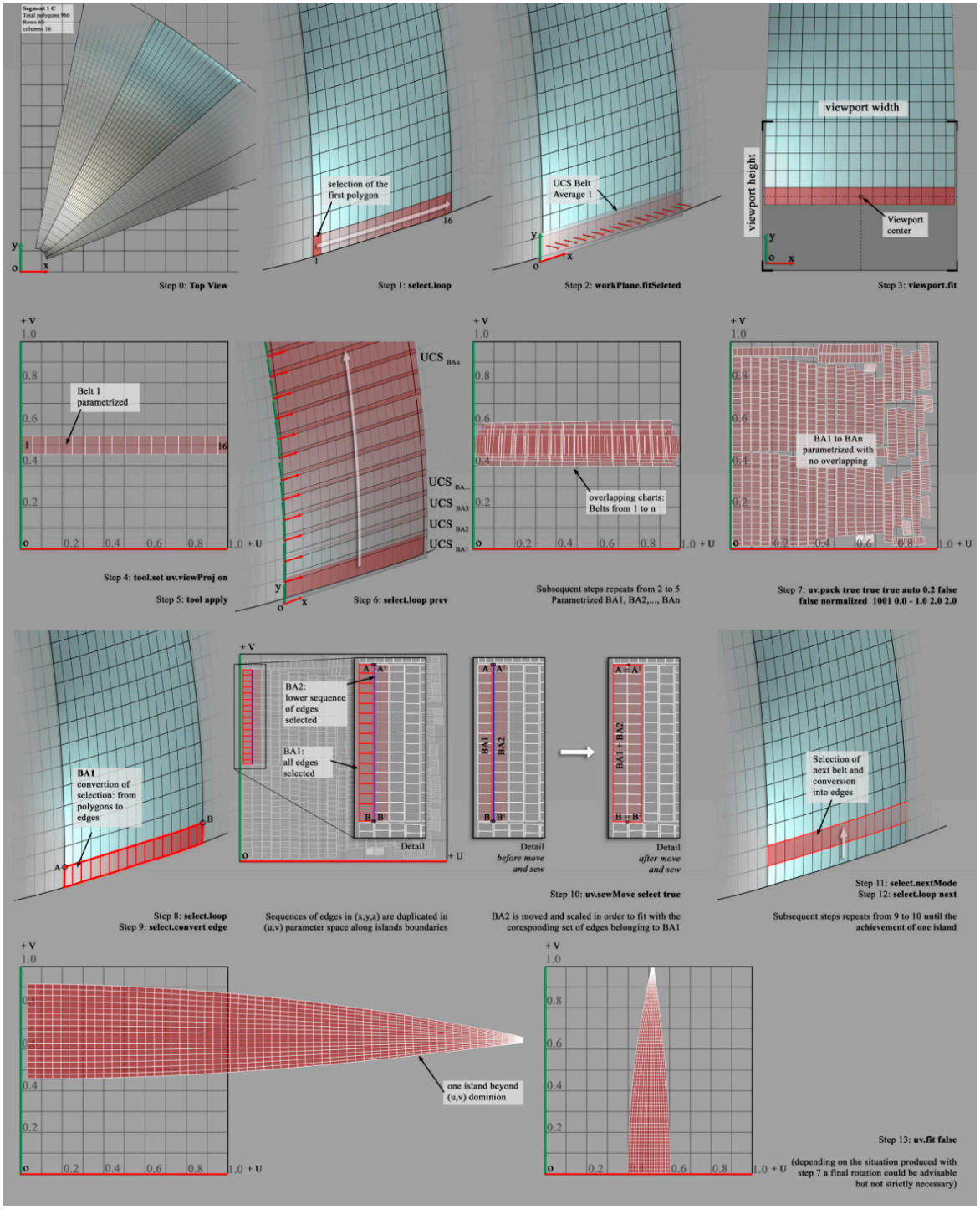

Figure 8. Automatic Multicenter Orthographic Projection (AMOP) script graphical description.

3.6. Associating Textures with Geometry Pseudo-Development

Execution of the above script allows parametrization of each section resulting by dome subdivision. Upon association of the UV map with each section, it is possible to import them into the photogrammetry software used for image modeling, subsequently allowing definition of image orientation parameters. In this environment, it is possible to import each section with the associated UV map and recalculate model textures based on the new (u,v) map, which effectively acts as the pseudo-development by projection of geometry and texture [31].

The final step allows scaling of the (u,v) map, defined in the image space by coordinates ranging from 0 to 1, against the actual dimensions of boundary representation. For this purpose, boundary lines of the sections—derived by geometry development—are defined as reference for image scaling.

4. Results and Discussion

The accuracy of geometry development was checked by comparing, in each zone, the boundary length on the original 3D model and on projections obtained either with the Rhinoceros software or by scaling the (u,v) map at real dimensions. Results, shown in Table 1, are compatible with the 1:100 project scale and in some cases, with definitely greater scales. In Table 1, the following zones are checked:

Table 1. Accuracy assessment of boundary representation planar development. La: length of left zone's boundary along meridian direction measured on the original 3D model. Ld: length of the bottom zone's boundary along horizontal direction measured on the original 3D model. Las: length of left zone's boundary along meridian direction measured on planar projection. Lds: length of the bottom zone's boundary along horizontal direction measured on planar projection.

Boundary Segment / Zone	La [m]	Las [m]	La-Las [m]	Ld [m]	Lds [m]	Ld-Lds [m]
R1	14.014	14.013	0.002	2.356	2.351	0.005
R2	13.954	13.954	0.000	0.304	0.304	0.000
R3	14.053	14.053	0.000	1.059	1.058	0.001
R4	13.932	13.932	0.000	0.529	0.529	0.000
S2A	13.987	14.002	−0.015	1.825	1.806	0.019
S2B	14.109	14.104	0.005	2.263	2.257	0.007
S2C	14.281	14.280	0.001	2.044	2.033	0.011
S3A	14.456	14.465	−0.010	1.505	1.501	0.004
S3B	14.440	14.443	−0.002	3.905	3.882	0.023
S4A	14.261	14.269	−0.008	0.834	0.834	0.000
S4B	14.212	14.210	0.001	2.174	2.170	0.004
S5A	13.930	13.942	−0.012	1.893	1.890	0.003
S5B	13.676	13.688	−0.012	1.744	1.746	−0.001
S5C	13.559	13.563	−0.004	1.975	1.975	0.000
S5D	13.631	13.629	0.002	2.010	2.000	0.010
S6A	14.007	14.006	0.001	2.086	2.070	0.016
S6B	14.225	14.217	0.008	1.474	1.473	0.001
S6C	14.318	14.310	0.008	1.975	1.968	0.007
S7A	14.412	14.421	−0.009	0.622	0.618	0.004
S7B	14.423	14.438	−0.015	3.104	3.103	0.000
S8A	14.396	14.404	−0.008	0.896	0.895	0.000
S8B	14.333	14.346	−0.012	2.959	2.941	0.018
S8C	14.084	14.086	−0.002	0.750	0.748	0.002

Figure 9 shows a collage of the pseudo-developments by projection of the regions in which the dome of Pisa Cathedral was divided. Considering the accuracy of the 3D survey, image resolution, the extension of the single regions, and the checks performed on geometry, the collage is suitable for 1:100 printing.

Achieving large scales depends solely on reducing region size and is therefore attained by dividing the model into a greater number of regions. At greater scales, this kind of document can provide restorers with on-site support for the reconstruction of frescoed domes. The availability of such archive documentation allows reconstruction of damaged frescoes while ensuring full respect of original geometries.

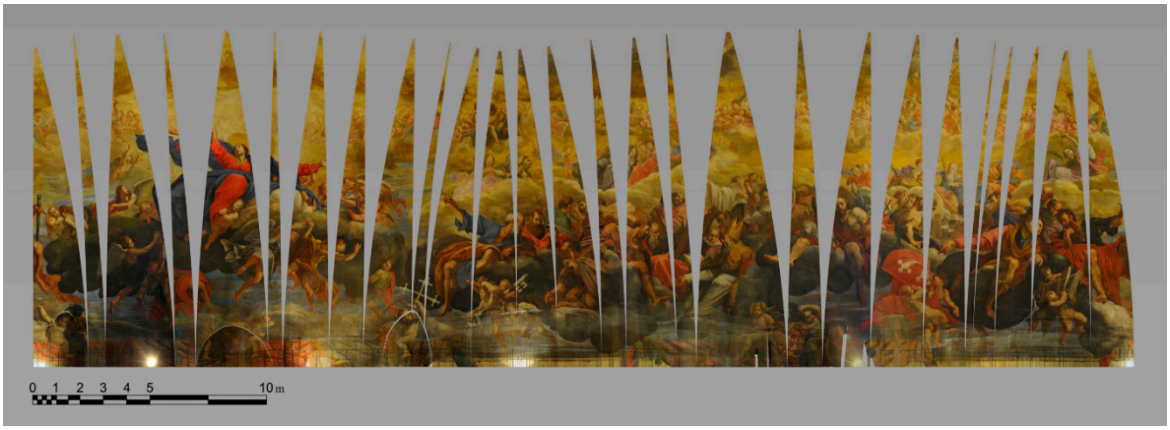

Figure 9. Pseudo-development by projection of the Pisa Cathedral dome.

By analyzing the pseudo-development, representation of the portion closer to the dome impost is relatively continuous due to the comparatively great extensions of the regions. On the other hand, planar representation of the fresco portion closer to the dome summit is quite fragmented due to the limited extension of the regions.

A similar problem is also found in cartographic projections where, in order to prevent excessive fragmentation, latitudes ranging up to 70°–80° N use the Transverse Mercator projection, while polar caps use stereographic polar projection.

This could also be effectively used for the representation of the summit portion of domes, since it allows an easier, more continuous view of frescoed areas. The enhancement of the methodology described incorporating these suggestions will be the object of future investigations.

5. Conclusions

The methodology described (shown using a flow chart in Figure 10) allowed pseudo-development by projection of the fresco painted on an oval dome, which provides the more inclusive example of vaulted or domed surfaces due to the complexity and curvature variability of its sections.

As regards surveying methodology, integrating TLS and photogrammetry enabled the best exploitation of their respective strengths, i.e., homogeneous geometric accuracy and color quality.

The pseudo-development required solving the problem of processing surfaces not approximated by a developable primitive using a polycentric orthographic azimuthal projection, dividing the dome into fuses and bands. The sections delimiting the fuses were defined considering the required representation scale, which limited the width of the regions, along with the defining sections related to the building methodology and the analysis of the Gaussian curvature. Bands were defined by identifying the normal of the different projection planes via a custom AMOP script.

In fact, a good portion of the originality of the present methodology lies in this script, which allows, via the projection of geometry in the (u,v) space, the achievement of the planar representation not only of geometric shapes but also of the texture associated with the 3D model.

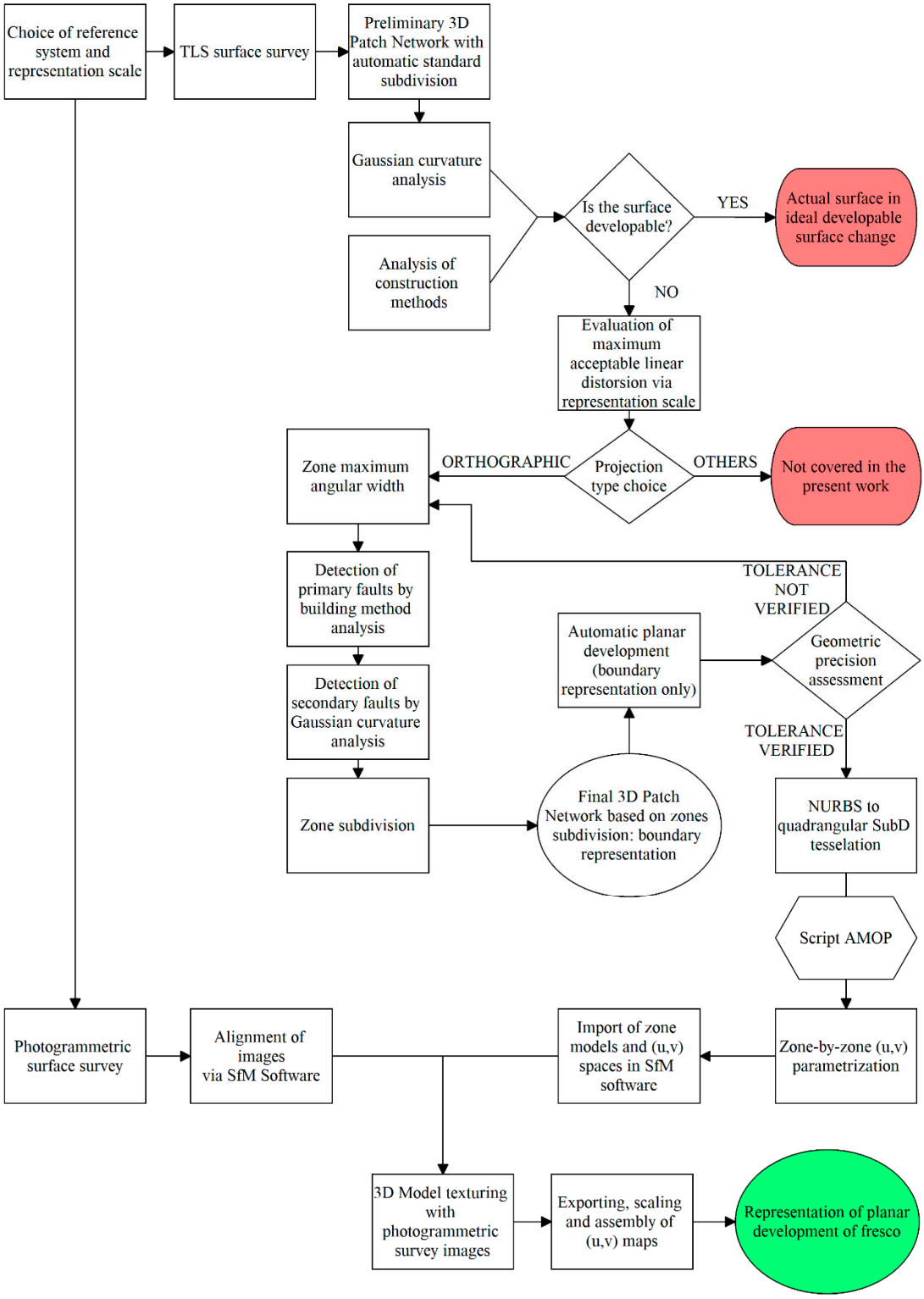

Figure 10. Flow chart of the methodology suggested.

Author Contributions: Conceptualization, A.P. and F.F.; Data curation, A.P., G.C., I.M.-E.Z., F.F., and L.C.; Funding acquisition, A.P. and G.C.; Investigation, A.P., G.C., and I.M.-E.Z.; Methodology, A.P., G.C., F.F., and L.C.; Software, F.F.; Supervision, A.P.; Validation, A.P., I.M.-E.Z., and F.F.; Visualization, I.M.-E.Z., and F.F.; Writing—Original Draft, A.P., G.C., I.M.-E.Z., F.F., and L.C.; Writing—Review & Editing, A.P., G.C., I.M.-E.Z., F.F., and L.C.

Funding: This research was partially funded by Università di Pisa grant number PRA_2017_12.

Acknowledgments: Thanks are due to Opera Primaziale Pisana for granting the required authorizations for the survey of the Pisa Cathedral dome; Eurotec Pisa srl for collaboration throughout the survey; technical staff members Andrea Bedini and Jessica Micheloni for survey execution.

Conflicts of Interest: The authors declare no conflict of interest. The funders had no role in the design of the study; in the collection, analyses, or interpretation of data; in the writing of the manuscript; and in the decision to publish the results.

References

1. Robleda, P.G.; Caroti, G.; Martínez-Espejo Zaragoza, I.; Piemonte, A. Computational vision in UV-mapping of textured meshes coming from photogrammetric recovery: Unwrapping frescoed vaults. *ISPRS Int. Arch. Photogramm. Remote Sens. Spat. Inf. Sci.* **2016**, *XLI-B5*, 391–398. [CrossRef]
2. Caroti, G.; Martínez-Espejo Zaragoza, I.; Piemonte, A. Range and image based modelling: A way for frescoed vault texturing optimization. *ISPRS Int. Arch. Photogramm. Remote Sens. Spat. Inf. Sci.* **2015**, *XL-5/W4*, 285–290. [CrossRef]
3. Chiabrando, F.; Rinaudo, F. Recovering a collapsed medieval fresco by using 3D modeling techniques. *ISPRS Ann. Photogramm. Remote Sens. Spat. Inf. Sci.* **2014**, *II-5*, 105–112. [CrossRef]
4. Bevilacqua, M.G.; Caroti, G.; Piemonte, A.; Ruschi, P.; Tenchini, L. 3D survey techniques for the architectutal restoration: The case of St. Agata in Pisa. *ISPRS Int. Arch. Photogramm. Remote Sens. Spat. Inf. Sci.* **2017**, *XLII-5/W1*, 441–447. [CrossRef]
5. Clini, P.; Frontoni, E.; Quattrini, R.; Pierdicca, R. Augmented Reality Experience: From High-Resolution Acquisition to Real Time Augmented Contents. *Adv. Multimed.* **2014**, *2014*, 597476. [CrossRef]
6. Sammartano, G.; Spanò, A. High scale 3D modelling and orthophoto of curved masonriesfor a multipurpose representation, analysis and assessment. *ISPRS Int. Arch. Photogramm. Remote Sens. Spat. Inf. Sci.* **2017**, *XLII-5/W1*, 245–252. [CrossRef]
7. Rieck, B.; Mara, H.; Krömker, S. Unwrapping highly-detailed 3d meshes of rotationally symmetric man-made objects. *ISPRS Ann. Photogramm. Remote Sens. Spat. Inf. Sci.* **2013**, *II-5/W1*, 259–264. [CrossRef]
8. Carli, E. *Il Duomo Di Pisa. Collana Chiese Monumentali d'Italia*; Nardini Collana: Firenze, Italy, 1989.
9. Sanpaolesi, P. Il restauro delle strutture della cupola della Cattedrale di Pisa. *Bolletino d'Arte* **1959**, *44*, 199–230.
10. Venditelli, L. *Il Mausoleo Di Sant'Elena. Gli Scavi*; Mondadori Electa: Firenze, Italy, 2011.
11. Rakob, F. Römische Kuppelbauten in Baiae. In *Mitteilungen Des DeutschenArchäologischenInstituts*; Römische Abteilung: Mainz, Germany, 1988.
12. Cipriani, L.; Fantini, F.; Bertacchi, S. The Geometric Enigma of Small Baths at Hadrian's Villa: Mixtilinear Plan Design and Complex Roofing Conception. *Nexus Netw. J.* **2017**, *19*, 427–453. [CrossRef]
13. WardPerkins, J.B. *Architettura Romana*; Mondadori Electa: Firenze, Italy, 1974.
14. Aita, D.; Barsotti, R.; Bennati, S.; Caroti, G.; Piemonte, A. 3-dimensional geometric survey and structural modelling of the dome of Pisa cathedral. *ISPRS Int. Arch. Photogramm. Remote Sens. Spat. Inf. Sci.* **2017**, *XLII-2/W3*, 39–46. [CrossRef]
15. Guidi, G.; Remondino, F. 3D Modelling from Real Data. In *Modeling and Simulation in Engineering*; InTech: Munich/Garching, Germany, 2012. [CrossRef]
16. Remondino, F.; Spera, M.G.; Nocerino, E.; Menna, F.; Nex, F. State of the art in high density image matching. *Photogramm. Rec.* **2014**, *29*, 144–166. [CrossRef]
17. Karras, G.E.; Patias, P.; Petsa, E. Digital monoplotting and photo-unwrapping of developable surfaces in architectural photogrammetry. *Int. Arch. Photogramm. Remote Sens.* **1996**, *31*, 290–294.
18. Karras, G.E.; Patias, P.; Petsa, E.; Ketipis, K. Raster projection and development of curved surfaces. *Int. Arch. Photogramm. Remote Sens.* **1997**, *XXXII*, 179–185.
19. Verhoeven, G.J.; Missinne, S.J. Unfolding leonardo da Vinci's globe (AD 1504) to reveal its historical world map. *ISPRS Ann. Photogramm. Remote Sens. Spat. Inf. Sci.* **2017**, *IV-2/W2*, 303–310. [CrossRef]
20. Grafarend, E.W.; Krumm, F.W. *Map Projections*; Springer: Berlin/Heidelberg, Germany, 2006.
21. Massarwi, F.; Gotsman, C.; Elber, G. Papercraft Models using Generalized Cylinders. In Proceedings of the 15th Pacific Conference on Computer Graphics and Applications (PG'07), Maui, HI, USA, 29 October–2 November 2007; pp. 148–157.

22. Bevilacqua, M.; Caroti, G.; Martínez-Espejo Zaragoza, I.; Piemonte, A. Frescoed Vaults: Accuracy Controlled Simplified Methodology for Planar Development of Three-Dimensional Textured Models. *Remote Sens.* **2016**, *8*, 239. [CrossRef]
23. Ciarloni, R. La logica delle forme. In *La Ricerca Nell'ambito Della Geometria Descrittiva*; Gangemi: Roma, Italy, 2016.
24. Gaiani, M. *La Rappresentazione Riconfigurata. Un Viaggio Lungo Il Processo Di Produzione Del Progetto Di Disegno Industriale*; POLI. Design: Milan, Italy, 2006.
25. Lai, Y.-K.; Kobbelt, L.; Hu, S.-M. An incremental approach to feature aligned quad dominant remeshing. In Proceedings of the 2008 ACM Symposium on Solid and Physical Modeling (SPM'08), Stony Brook, NY, USA, 2–4 June 2008; p. 137.
26. Jakob, W.; Tarini, M.; Panozzo, D.; Sorkine-Hornung, O. Instant field-aligned meshes. *ACM. Trans. Graph.* **2015**, *34*, 1–15. [CrossRef]
27. Shen, J.; Kosinka, J.; Sabin, M.; Dodgson, N. Converting a CAD model into a non-uniform subdivision surface. *Comput. Aided Geom. Des.* **2016**, *48*, 17–35. [CrossRef]
28. Valerio, V. La forma dell'ellisse. In *Arte e Matematica: Un Sorprendente Binomio*; Arte Tipografica: Napoli, Italy, 2006; pp. 241–262.
29. Scalzo, M.S. Agata a Pisa. In *Rotonde d'Italia. Analisi Tipologica Della Pianta Centrale*; Volta Valentino: Milano, Italy, 2008.
30. Filkins, P.C.; Tuohy, S.T.; Patrikalakis, N.M. Computational methods for blending surface approximation. *Eng. Comput.* **1993**, *9*, 49–62. [CrossRef]
31. Verhoeven, G.J. Computer graphics meets image fusion: The power of texture baking to simultaneously visualise 3D surface features and colour. *ISPRS Ann. Photogramm. Remote Sens. Spat. Inf. Sci.* **2017**, *IV-2/W2*, 295–302. [CrossRef]